CRYSTAL GROWTH & DESIGN

Article

pubs.acs.org/crystal

A Comparison of the Crystallization Inhibition Properties of Bile Salts

Na Li,[†] Laura I. Mosquera-Giraldo,[†] Carlos H. Borca,[‡] James D. Ormes,[§] Michael Lowinger,[∥] John D. Higgins,[⊥] Lyudmila V. Slipchenko,[‡] and Lynne S. Taylor*[,†]

[†]Department of Industrial and Physical Pharmacy, Purdue University, 575 Stadium Mall Drive, West Lafayette, Indiana 47907, United States

[‡]Department of Chemistry, College of Science, Purdue University, West Lafayette, Indiana 47907, United States

[§]Discovery Pharmaceutical Sciences, Merck Research Laboratories, Merck & Co., Inc., Rahway, New Jersey 07065, United States

[∥]Formulation Sciences, Merck Research Laboratories, Merck & Co., Inc., Kenilworth, New Jersey 07033, United States

[⊥]Discovery Pharmaceutical Sciences, Merck Research Laboratories, Merck & Co., Inc., West Point, Pennsylvania 19846, United States

Supporting Information

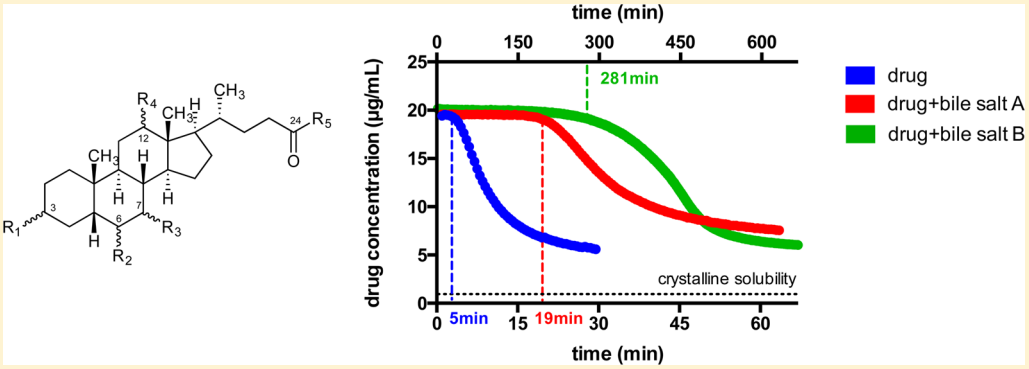

ABSTRACT: Bile salts are natural surfactants present in the human gastrointestinal tract. Therefore, it is essential to consider their effect on the dissolution and crystallization tendency of oral drug formulations. Although a recent study showed that sodium taurocholate delayed nucleation for 11 structurally diverse compounds, there is limited information about the crystallization inhibition properties of other bile salts and whether they are interchangeable in this context. In this study, we evaluated the ability of 13 bile salts to maintain supersaturated aqueous solutions of three compounds: celecoxib, nevirapine, and fibanserin. Most bile salts extended nucleation induction times. However, their inhibitory effects varied depending on the structure and concentration of the bile salt and the drug. The R5 group and hydrophobicity of the bile salt appeared to be essential. Molecular dynamics simulations indicated that van der Waals and hydrogen bonding interactions occurred between nevirapine and bile salts, with variations in different systems. These results are important to better understand the crystallization tendency of orally delivered poorly water-soluble compounds in vivo.

INTRODUCTION

Permeability and solubility are two key characteristics in intestinal drug absorption;[1] for compounds with adequate permeability, solubility becomes the rate-limiting step at the absorption site. Consequently, factors that impact intestinal drug concentrations, in particular, the kinetics of phase transitions such as dissolution or crystallization, are critical. Formulation strategies such as inclusion in surfactant micelles,[2] cyclodextrin complexation,[3] cosolvents,[4] nanocrystals,[5] and amorphous solid dispersions[6] have been widely employed to improve aqueous solubility. However, only an increase in the concentration of molecularly dissolved drug can lead to an enhanced permeation rate through a membrane.[7,8] Formulations that produce supersaturated solutions can thus enhance passive diffusion through the enterocytes and may provide improved bioavailability if crystallization is prevented.

Supersaturation, where the drug is molecularly dissolved in solution at a higher concentration than the equilibrium crystalline solubility, can be achieved by formulating a neutral drug in the form of an amorphous solid dispersion, or can occur when a weakly basic drug transitions from the stomach to intestines, undergoing a change in ionization state. Because of the inherent instability of supersaturated solutions, the drug often crystallizes, leading to a loss in concentration. Therefore, maintaining supersaturation in the human gastrointestinal (GI) tract is essential to achieve enhanced oral absorption of compounds with solubility limited bioavailability. Previous studies have mainly focused on using polymeric additives such as cellulose derivatives to inhibit nucleation,[9−12] and the role of small molecule nucleation inhibitors in the context of

Received: October 6, 2016
Published: October 18, 2016

DOI: 10.1021/acs.cgd.6b01470
Cryst. Growth Des. XXXX, XXX, XXX−XXX

Table 1. Chemical Structure, Physicochemical Properties, and Liquid Media Used for Bile Salts

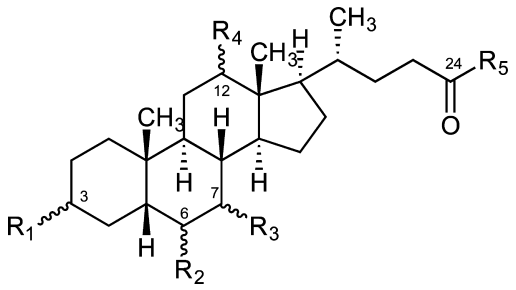

bile salts	abbreviation	R1	R2	R3	R4	R5	CMC (mM)	pH[a]	% in human bile[65]	Log P'_A[b]	molecular weight
free bile salts											
sodium cholate	SC	OH(α)	H	OH(α)	OH(α)	O^-Na^+	5.90–7.30[56]	6.5	trace	1.1[67]	430.55
sodium deoxycholate	SDC	OH(α)	H	H	OH(α)	O^-Na^+	2.35–2.56[56]	6.5	trace	2.65[67]	414.55
sodium chenodeoxycholate	SCDC	OH(α)	H	OH(α)	H	O^-Na^+	4–9[68]	6.8[c]	trace	2.25[67]	414.55
sodium lithocholate	SLC	OH(α)	H	H	H	O^-Na^+	0.5–0.9[68]	10[d]		NA[e]	398.55
sodium ursodeoxycholate	SUDC	OH(α)	H	OH(β)	H	O^-Na^+	7–19[68]	10[d]		2.20[67]	414.55
sodium hyodeoxycholate	SHDC	OH(α)	OH(α)	H	H	O^-Na^+	6–14[68]	10[d]		2.28[67]	414.55
glycine conjugated											
sodium glycocholate	SGC	OH(α)	H	OH(α)	OH(α)	$NHCH_2COO^-Na^+$	5.90–11.90[56]	6.5	30	−0.40[67]	487.60
sodium glycodeoxycholate	SGDC	OH(α)	H	H	OH(α)	$NHCH_2COO^-Na^+$	2.20–2.23[56]	6.5	15	0.80[67]	471.61
sodium glycochenodeoxycholate	SGCDC	OH(α)	H	OH(α)	H	$NHCH_2COO^-Na^+$	1.5–2.6[69]	6.5	30	0.45[67]	471.61
sodium glycoursodeoxycholate	SGUDC	OH(α)	H	OH(β)	H	$NHCH_2COO^-Na^+$	>5[69]	10[d]		0.20[67]	471.61
taurine conjugated											
sodium taurocholate	STC	OH(α)	H	OH(α)	OH(α)	$NHCH_2\ CH_2SO_3^-Na^+$	3–5[70]	6.5	10	−0.50[67]	537.69
sodium taurodeoxycholate	STDC	OH(α)	H	H	OH(α)	$NHCH_2\ CH_2SO_3^-Na^+$	2.0–2.9[70]	6.5	10	NA[e]	521.69
sodium taurochenodeoxycholate	STCDC	OH(α)	H	OH(α)	H	$NHCH_2\ CH_2SO_3^-Na^+$	1.3–2.7[69]	6.5	5	NA[e]	521.69

[a]pH 6.5, 6.8, and 8: 50 mM sodium phosphate buffer. pH 10: 50 mM sodium carbonate buffer. [b]Experimentally determined partition coefficient of the ionized bile acids. [c]Not soluble in pH 6.5 buffer at 37 °C. [d]Not soluble in pH 8 buffer at 37 °C. [e]NA: Not available.

DOI: 10.1021/acs.cgd.6b01470
Cryst. Growth Des. XXXX, XXX, XXX−XXX

maintaining supersaturation for oral drug delivery has not been widely explored.

Bile salts are a group of naturally occurring surfactants present in the human GI tract. Bile salts are steroid derivatives and exhibit facial polarity, whereby the hydroxyl groups are predominantly present on one side of the molecule, while nonpolar groups are present on the other side.[13] The structures of 13 bile salts are shown in Table 1. Sodium taurocholate (STC) is widely used in biorelevant dissolution media as a model bile salt.[14] In a recent study, it was shown that STC was able to inhibit crystallization, extending nucleation induction times for a group of structurally diverse compounds.[15] It was also noted that two other bile salts, sodium glycocholate (SGC) and sodium glycodeoxycholate (SGDC), demonstrated nucleation inhibitory effects toward celecoxib and nevirapine.[15] However, there is limited information about the crystallization inhibition properties of other bile salts and whether they are interchangeable in terms of their ability to inhibit nucleation. This is important to predict the tendency for drug precipitation in vivo based on in vitro tests. It has been observed that in vitro tests tend to overestimate the extent of precipitation observed in vivo.[16] Several factors may contribute to these observations. First, the gastrointestinal tract is a dynamic system in which dilution is constantly occurring, while in vitro tests are typically conducted under static conditions with a fixed concentration. Second, the current biorelevant medium used to evaluate the crystallization tendency in in vitro tests might be oversimplified. Therefore, the goal of this study was to evaluate the ability of a group of 13 bile salts to delay nucleation from supersaturated solutions of poorly water-soluble compounds. Celecoxib was chosen as a model neutral compound over the physiological pH range. Nevirapine and flibanserin were selected as model weak bases with pK_a values lower than 6.5. The results indicate that the ability to inhibit crystallization depends on the chemistry of the bile salt and that its selection is critical when evaluating supersaturating dosage forms in biorelevant dissolution media.

MATERIALS AND METHODS

Materials. Celecoxib (Figure 1) and flibanserin (Figure 1) were purchased from Attix Pharmaceuticals (Toronto, ON, Canada).

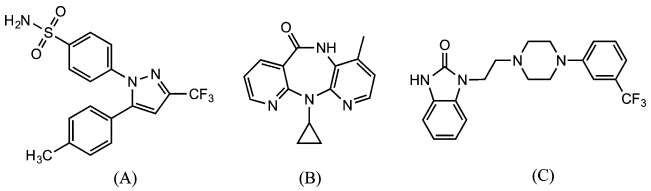

Figure 1. Molecular structures of (A) celecoxib, (B) nevirapine, and (C) flibanserin.

Nevirapine (Figure 1) was purchased from Chempacific (Baltimore, MD). Bile salts and bile acids (Table 1), including sodium cholate (SC), sodium deoxycholate (SDC), sodium chenodeoxycholate (SCDC), lithocholic acid (LCA), ursodeoxycholic acid (UDCA), hyodeoxycholic acid (HDCA), sodium glycocholate (SGC), sodium glycodeoxycholate (SGDC), sodium glycochenodeoxycholate (SGCDC), glycoursodeoxycholic acid (GUDCA), sodium taurocholate (STC), sodium taurochenodeoxycholate (STCDC), and sodium taurodeoxycholate (STDC) were purchased from Sigma-Aldrich Co. (St Louis, MO, USA). Methanol, acetonitrile, and dimethyl sulfoxide (DMSO) were purchased from Macron Chemicals (Philipsburg, NJ, USA). 50 mM phosphate buffer solutions at different pH values were prepared using sodium phosphate dibasic anhydrous and sodium phosphate monobasic monohydrate (Macron, Chemicals, Philipsburg, NJ, USA). 50 mM pH 10 sodium carbonate solution was prepared using sodium carbonate and sodium bicarbonate (Sigma-Aldrich Co., St Louis, MO, USA).

50 mM pH 6.5 phosphate buffer was prepared by dissolving 2.236 g of sodium phosphate dibasic and 4.726 g of sodium phosphate monobasic monohydrate in water to a final volume of 1000 mL. 50 mM pH 6.8 phosphate buffer was prepared by dissolving 3.478 g of sodium phosphate dibasic and 3.519 g of sodium phosphate monobasic monohydrate in water to a final volume of 1000 mL. 50 mM pH 10 carbonate buffer was prepared by dissolving 2.915 g of sodium carbonate and 1.890 g of sodium bicarbonate in water to a final volume of 1000 mL. The final pH values of these solutions were also verified with a pH meter.

Methods. *Solubility Determination.* The equilibrium crystalline solubility of celecoxib, nevirapine, and flibanserin was determined in the presence and absence of bile salts in phosphate buffer. The solid state forms of these compounds upon completion of the solubility experiments in the presence and absence of STC were evaluated using X-ray powder diffraction and differential scanning calorimetry. No difference in the solid state form was observed in the presence and absence of STC. The solid state forms at the end of the solubility experiments were found to be celecoxib form III,[17] nevirapine anhydrous,[18] and flibanserin polymorph A.[19] Bile salts or acids were predissolved in 15 mL sodium phosphate buffer at a specified pH (Table 1) to ensure complete ionization and solubilization. An excess amount of the crystalline drug was added to the mixture and equilibrated at 37 °C using a water bath shaker. All samples were prepared in triplicate. For celecoxib and nevirapine, the mixture was incubated for 48 h. For flibanserin, the mixture was equilibrated for 1 h to minimize degradation. Upon incubation, the final pH values of selected solutions were checked using a pH meter. An Optima L-100XP ultracentrifuge (Beckman Coulter Inc., Brea, CA, USA) equipped with a swinging-bucket rotor SW 41Ti was used to separate the supernatant and the undissolved crystalline solids at 37 °C and 35 000 rpm for 30 min. The drug concentration in the supernatant was then determined by high performance liquid chromatography.

High Performance Liquid Chromatography (HPLC). An Agilent 1269/1290 Infinity Series HPLC system (Agilent Technologies, Santa Clara, CA, USA) was used along with Agilent Chemstation software. The separation column used was a Waters XTerra RP-18 column (100 mm × 4.6 mm i.d., 3.5 μm particle size).

For celecoxib, a mobile phase of 80% acetonitrile and 20% water (v/v) was used at a flow rate of 0.25 mL/min with an injection volume of 10 μL. The total run length was 10 min. The UV signal was detected at 258 nm. For samples dissolved in pH 10 buffer, a mobile phase of 80% acetonitrile and 20% water with 0.1% formic acid (v/v) was used to minimize ionization of the drug.

For nevirapine, the mobile phase used was 0.1% formic acid aqueous solution and acetonitrile at a 65:35 (v/v) ratio at 0.25 mL/min with an injection volume of 10 μL. The run length was 8 min. The UV signal was detected at 210 nm.

For flibanserin, a mobile phase A of 0.1% formic acid aqueous solution and mobile phase B of acetonitrile at 67:33 (v/v) ratio at 0.25 mL/min was used for a run length of 15 min, and the injection volume was 10 μL. The UV signal was detected at 247 nm.

Apparent Supersaturation. The apparent supersaturation ratio S' is commonly defined as[10]

$$S' = \frac{C}{C_s} \tag{1}$$

where C is the actual drug concentration in the supersaturated solution, and C_s is the equilibrium crystalline solubility of the drug in the presence of a bile salt at a concentration of 1 mg/mL (0.1% w/v).

Nucleation Induction Time Measurements. To be able to fully dissolve the bile salts, different pH values were employed for the induction time measurements, to promote dissociation of the bile salt to the ionized form. A pH value of 6.5 was used wherever possible to represent the physiological conditions in the human GI tract (the

DOI: 10.1021/acs.cgd.6b01470
Cryst. Growth Des. XXXX, XXX, XXX−XXX

duodenum).[20] However, higher pH solutions were used to fully dissolve bile acids with a pK_a value greater than 6.5 (Table 1).

The nucleation induction time is defined as the time after the creation of supersaturation when the first nuclei is formed.[21] For experimental measurements, the induction time (t_{ind}) was defined as the nucleation time for the critical nucleus to form (t_n) plus the time taken for the crystals to grow to a detectable size (t_g). However, direct measurement of true nucleation time is not experimentally possible, because the nuclei can only be detected when they grow to detectable sizes.[10] If $t_n \gg t_g$, then the induction time t_{ind} is dominated by the true nucleation time t_n. This assumption appears to hold true, and it is standard practice to measure induction times t_{ind} to better understand nucleation kinetics.[10,22−24]

Nucleation induction time measurements were performed using an SI photonics UV/vis spectrophotometer equipped with a fiber optic dip probe (Tuscon, AZ, USA). Different drugs have different solubility values and extinction coefficients, and hence different UV absorptivities were observed for the supersaturated solutions. In order to achieve adequate UV absorptions that were within the linear portion of the detection range (i.e., neither too high nor too low), different probe path lengths were used: 10 mm, 2 mm, and 5 mm for celecoxib, nevirapine, and flibanserin, respectively. Wavelength scans from 200 to 450 nm were obtained every 10−60 s. For celecoxib, the onset of crystal formation was determined from the decrease of drug concentration at 259 nm, where the drug has an absorption maximum. The onset time from measuring the change in absorption was found to correspond well with the increase in intensity of light scattering at 350 nm (extinction). Celecoxib has no absorption at this wavelength, and therefore, an increase in signal at this wavelength indicates that scattering species such as crystals are present. For nevirapine, the onset crystallization time was determined by monitoring light intensity changes at 334 nm (absorption, shoulder) and 400 nm (extinction). For flibanserin, the absorption and extinction wavelengths used were 280 and 350 nm, respectively. These wavelengths were chosen to represent spectral regions where the drugs either showed an absorption maximum or no absorption enabling the onset of crystallization to be detected by a loss of solution concentration and an increase in solution scattering, respectively.

For celecoxib, the stock solution was prepared by dissolving 100.2 mg of celecoxib in 10 mL methanol. 100 μL methanolic stock solution was then added to 50 mL of aqueous buffer solution with predissolved bile salts to generate a supersaturated celecoxib solution of 20 μg/mL. For nevirapine, the stock solution was prepared by dissolving 408 mg of nevirapine in 10 mL of DMSO. Nevirapine supersaturated solutions of 800 μg/mL were generated by adding 1 mL of the DMSO stock solution into 50 mL of aqueous buffer solutions containing bile salts. For flibanserin, 150.4 mg of solids were dissolved into 10 mL of methanol to make a stock solution. A total of 150 μL methanolic solution was then added into 50 mL of buffer to generate a 45 μg/mL supersaturated flibanserin solution. These drug concentrations were selected to be below their liquid−liquid phase separation (LLPS) values to avoid phase separation to a noncrystalline phase, yet supersaturated enough for crystallization to occur within a reasonable time frame. The solution was stirred at 300 rpm using a cross-shaped magnetic stirrer. A concentration of 1 mg/mL (0.1% w/v) was used for all bile salts unless specified elsewhere. For the nucleation induction time experiment with the six most prevalent human bile salts, 60 mg of SGC, 30 mg of SGDC, 60 mg of SGCDC, 20 mg of STC, 20 mg of STDC, and 10 mg of STCDC were weighed out and blended. The mixture was then added to pH 6.5 buffer solution to reach a final concentration of 1 mg/mL (0.1% w/v). UV wavelength scans started immediately after drug addition. All experiments were conducted at 37 °C in triplicate.

After the onset of nucleation, a decrease in solution concentration occurs due to desupersaturation caused by crystal growth. The rapid decrease in solution concentration is coupled with an increase in the intensity of light scattering, which is readily observable at a nonabsorbing wavelength. For celecoxib and flibanserin, the intersection of the regression lines for the two linear region of the absorption line was taken as the nucleation induction time.[10] For nevirapine, extrapolation was taken on the extinction line, due to interference in UV absorption from the high drug concentrations used.

Liquid−Liquid Phase Separation (LLPS) Concentration Determination. Drug stock solutions were titrated into 15 mL of 50 mM pH 6.5 sodium phosphate buffer solutions using a syringe pump (Harvard Apparatus, Holliston, MA, USA). The solutions were pre-equilibrated at 37 °C and stirred at 300 rpm. The LLPS concentration was determined as the point where the intensity of light scattering started to increase.[25] UV wavelength scans were performed at wavelengths from 200 to 450 nm. The time interval between scans was 10 s, with an addition rate of 40 μL/min for both celecoxib and flibanserin. For nevirapine, the time interval was 30 s, and the addition rate was 90 μL/min. An SI photonics UV/vis spectrophotometer coupled with a fiber optic dip probe (Tuscan, AZ, USA) was used. For celecoxib, the concentration of the methanol stock solution was 10 mg/mL, and the path length of the UV probe was 5 mm. For nevirapine, the concentration of the DMSO stock solution was 40 mg/mL, and the path length for the UV probe used was 2 mm. The methanolic stock solution used for flibanserin was 15 mg/mL, and the UV probe used was a 10 mm path length probe. All experiments were performed in triplicate.

Determination of Surfactant Critical Micelle Concentration (CMC). The CMCs (aggregation numbers) of STC and SGC in the presence of celecoxib were measured using the commonly employed approach of measuring COX crystal solubility as a function of surfactant concentration. An excess amount of crystalline COX was added to 10 mL pH 6.5 buffer solutions with various amounts of STC or SGC. After incubation for 48 h at 37 °C, the mixture was centrifuged using an Optima L-100XP ultracentrifuge (Beckman Coulter Inc., Brea, CA) coupled with a SW 70.1Ti rotor at 35 000 rpm for 30 min at 37 °C. One milliliter of the supernatant was then taken for HPLC analysis. The CMC value was determined by taking the intercept of the two linear portions of the plot.

Determination of Diffusion Rates. A side-by-side diffusion cell (PermeGear, Inc. Hellertown, PA) was used to determine the membrane transport rate and therefore to assess the impact of the bile salt on the supersaturation of the solution. A regenerated cellulose membrane with a molecular weight cutoff of 6−8 kDa was used to separate the donor and receiver side chambers. The diameter of the orifice connecting two chambers is 30 mm. Each chamber was filled with 34 mL of 50 mM pH 6.5 phosphate buffer solutions, with predissolved bile salts at a concentration of 0.1% (w/w). For experiments without bile salts, diffusion studies were run with and without HPMCAS MF (5 μg/mL) to confirm that no crystallization occurred over the course of the experiment; no difference in mass flow rates were observed for these two systems. The diffusion cell was maintained at 37 °C using a circulation water bath. Solutions on both sides were stirred at 300 rpm.

Initial donor drug concentrations were 20 μg/mL and 800 μg/mL for celecoxib and nevirapine, respectively. The concentration evolution of the drug on the receiver side was monitored using a fiber optic dip probe with an SI photonics UV/vis spectrophotometer (AZ, USA) with a path length of 20 mm. Concentrations versus time plots were generated, and the slope of the linear portion of the plot was taken as the mass flow rate in ng/s. The diffusive flux was calculated by dividing the mass flow rate with the surface area of the orifice.

Diffusion experiments with the pure drug without polymer were also conducted. A total of 300 μL of the donor solution were taken every 30 s or every 10 s for celecoxib and nevrapine for a total time of 5 and 2 min, respectively. Drug concentrations were determined using HPLC. The crystalline solubility values of celecoxib and nevirapine in the absence and presence of the polymer at 5 μg/mL were measured using the methods described in the Solubility Determination section.

Assuming sink conditions in the receiver cell, the diffusive flux, J, can be described using the following equation:

$$J = \frac{dM}{A \times dt} = \frac{Da}{h\gamma_m} \quad (2)$$

where the flux (J) is given by the mass flow rate (dM/dt) per unit membrane cross-sectional area (A). This depends on the solute

DOI: 10.1021/acs.cgd.6b01470
Cryst. Growth Des. XXXX, XXX, XXX−XXX

diffusion coefficient (D), the solute thermodynamic activity (a), the activity coefficient of the solute in the membrane (γ_m), and the thickness of the membrane (h). A, D, γ_m, and h are constants for a given experimental setup and solute. Hence the mass flow rate is directly proportional to the solute activity in the donor cell, and diffusion cell experiments can be used to evaluate whether the bile salts impact the supersaturation at a given added drug concentration and hence how well the supersaturation is approximated by eq 1.

Molecular Dynamics Simulations. To provide insight into the interaction between drug and bile salt, atomistic MD simulations were carried out in GROMACS 5.0,[27,28] using the CHARMM force field.[29,30] The model compound chosen was nevirapine, and four bile salts: SC, SDC, SHDC, and SUDC. The simulations were executed in five steps:

(1) First, the crystalline structure of nevirapine[31] and SC[32] was extracted from the Cambridge Structural Database. Then, in order to obtain SDC, SHDC, and SUDC bile salts, the structure of SC was modified using IQmol 2.7.1.[33]

(2) The structures were optimized with density functional theory at the PBE0/6-311++G** level of theory, using the Q-Chem 4.3[34] computational chemistry package. Then the structures were submitted to the online topology building tool SwissParam[35] to obtain topology files in GROMACS format.

(3) Dimers of bile salt and nevirapine were positioned in cubic boxes with 4.0 nm side length. Next, these dimers were solvated with 2100 water molecules of the extended simple point charge (SPC/E) water model. One Na^+ ion was added as a mobile counterion of the carboxylate group. Tetramers, including two molecules of bile salt and two drug molecules, were placed in cubic boxes with 6.0 nm side length, also containing 7020 water molecules, and 2 Na^+ were added.

(4) The time evolution of these systems was simulated using the velocity-Verlet algorithm with a time step of 1 fs. Periodic boundary conditions with the Verlet cutoff scheme were used. van der Waals forces interactions were calculated until a 1 nm cutoff. Electrostatic interactions were separated in a short-range computed up to a 1 nm and a long-range estimated with the particle mesh Ewald (PME) method.

(5) Each system was allowed to evolve for 100 ns in the canonical ensemble (NVT), using the v-rescale thermostat, at a reference temperature of 310 K, with a coupling constant (tau-t) of 0.2 ps. A total of 2000 equally separated snapshots (every 50 ps) were extracted for further analysis.

(6) The number of intermolecular hydrogen bonds along the trajectory was calculated using the visualization package VMD.[36] All possible hydrogen bond donors and acceptors were taken into account. The hydrogen bond was defined using a distance and angle cut-offs of 3.0 Å and 20°, respectively.

(7) The number of clusters along the trajectory was computed using GROMACS. Molecules were considered as a part of the same cluster if the intermolecular distance was equal or less than 3.0 Å.

RESULTS

Physicochemical Properties of the Model Compounds. Celecoxib, nevirapine, and flibanserin, shown in Figure 1, were selected as three model compounds to represent structurally diverse, poorly water-soluble drugs. Celecoxib is a weak acid with a pK_a of 11.1,[37] nevirapine is a weak base, with a pK_a of 2.8,[38] and flibanserin is also a weak base, with a pK_a of 5.9 at 25 °C.[39] Thus, over the pH range of the human intestinal environment, these drugs are mostly in their un-ionized free forms. The high log P values and melting points of these compounds (Table 2) suggest that they will be poorly soluble in aqueous media.

The equilibrium solubility values of crystalline celecoxib, nevirapine, and flibanserin at 37 °C and different pH conditions, with or without the presence of bile salts, are shown in Table 3; all compounds have low aqueous solubility. The final pH values of selected solutions are also shown; these were taken at the end of the solubility measurements. The crystal solubility of celecoxib and flibanserin was slightly enhanced at the concentration of the bile salts evaluated, but no change was seen for nevirapine (Table 3). Celecoxib has a reported acidic pK_a of 11.1 (Table 2), and a greater extent of solubilization was observed in the presence of bile salts at pH 10 (Table 3). This could be due to a small extent of ionization (about 7.5% of celexcoxib is expected to be ionized at this pH). Changing the buffer might also contribute to differences in the observed solubilization values. For flibanserin, which has a pK_a of 5.9, 80% of the drug is expected to be un-ionized at pH 6.5. At the higher pH values, the compounds will be >99.9% un-ionized. However, no clear trends can be observed in the extent of solubilization for the different bile salts at the different pH values. Nevirapine is a very weak base with a pK_a value of 2.8 (Table 2), and hence within the pH range used in this study, negligible ionization is expected. Interestingly, for flibanserin, insoluble complex formation was observed with SDC, SCDC, and SLC. This might be due to the partial ionization of this molecule and consequently the formation of insoluble salts with the negatively charged bile salts.[40]

Table 2. Physicochemical Properties of Model Compounds

property	celecoxib	nevirapine	flibanserin
pK_a	11.1[37]	2.8[38]	5.9[39]
molecular weight (g/mol)	381.37	266.30	390.40
log P[a]	4.34	2.05	3.47
melting point (°C)	163.5[10]	244.4	128.9
crystalline solubility (μg/mL)	1.2 ± 0.1	105.3 ± 5.1	9.4 ± 1.9
LLPS (μg/mL)	42.8 ± 4.2	874 ± 106	57.3 ± 2.1

[a]Log P values were obtained from ChemBioDraw Ultra 14.0.

Nucleation Induction Times. The effect of 13 bile salts on the nucleation induction time of celecoxib, nevirapine, and flibanserin was tested. The antinucleation effect of bile salts was inferred from drug nucleation induction time measurements, summarized in Table 4.[10] It is apparent that most bile salts delayed nucleation of the three compounds, as indicated by extended induction times relative to values obtained in the absence of bile salts. In other words, the supersaturated solutions persisted for longer durations relative to the absence of the bile salts, where desupersaturation was very rapid. However, the antinucleation effect of different bile salts toward the same compound varied greatly. For celecoxib, most bile salts led to longer nucleation induction times compared to the buffer control, except for systems with SGDC and STDC. For nevirapine, all bile salts exhibited antinucleation effects except for SLC. Upon addition of nevirapine to this solution, insoluble particles were formed. This may suggest the formation of an insoluble compound, although SLC did not alter the crystalline solubility of nevirapine (Table 3). For flibanserin, STDC was not effective, while SDC, SCDC, and SLC formed insoluble particles with flibanserin. Further investigation of these insoluble species is needed to better understand their structure.

The most effective nucleation inhibitors for celecoxib were SDC and STCDC, followed by SC and SGC. For nevirapine, SHDC and SDC were superior, followed by STCDC, and then SCDC and SGC. For flibanserin, STCDC, SHDC, SGUDC, and SGC were the top four nucleation inhibitors. Interestingly, the same bile salt exerted different antinucleation effects with different drug molecules. For example, SC was a good nucleation inhibitor for celecoxib, yet it exhibited only relatively modest inhibitory effects on nevirapine and flibanserin

DOI: 10.1021/acs.cgd.6b01470
Cryst. Growth Des. XXXX, XXX, XXX−XXX

Table 3. Equilibrium Solubility Values of Model Compounds[a]

		solubility (μg/mL)		
system	media pH	celecoxib	nevirapine	flibanserin
pH 6.5 buffer	6.5	1.2 ± 0.1	105.3 ± 5.1	9.4 ± 1.9
free bile salts				
SC	6.5	3.0 ± 0.1	103.9 ± 1.4	13.6 ± 3.7
SDC	6.5	3.1 ± 0.1	101.3 ± 4.7	0.5 ± 0.2[c] (6.50 ± 0.01)
SCDC	6.8	3.14 ± 0.03	105.0 ± 4.0	3.6 ± 1.0[c] (6.797 ± 0.006)
SLC	10	7.7 ± 0.3[b] (9.967 ± 0.006)	99.3 ± 1.1	0.1 ± 0.1[c] (9.91 ± 0.02)
SUDC	10	9.4 ± 0.8[b] (9.96 ± 0.03)	110.9 ± 2.8	14.0 ± 4.2
SHDC	10	10.6 ± 0.3[b] (9.96 ± 0.04)	91.8 ± 2.11	13.0 ± 3.1
glycine conjugated				
SGC	6.5	3.5 ± 0.6	102.0 ± 0.6	15.2 ± 4.2
SGDC	6.5	2.8 ± 0.1	102.8 ± 0.4	8.1 ± 1.9
SGCDC	6.5	3.2 ± 0.1	108.6 ± 8.3	11.6 ± 2.9
SGUDC	10	11.1 ± 0.6[b] (9.97 ± 0.01)	110.0 ± 0.7	14.4 ± 4.1
taurine conjugated				
STC	6.5	2.9 ± 0.2 (6.503 ± 0.006)	100.5 ± 2.1 (6.51 ± 0.00)	14.9 ± 3.3 (6.503 ± 0.006)
STDC	6.5	2.7 ± 0.1	103.1 ± 1.2	9.4 ± 1.2
STCDC	6.5	3.340 ± 0.003	112.5 ± 3.1	9.1 ± 2.8

[a]The final pH values of selected solutions are shown in parentheses. [b]Ionization led to greater extent of solubilization. [c]Insoluble compounds were formed.

Table 4. Nucleation Induction Times for Model Compounds with 0.1% (w/v) Bile Salts at 37 °C

	induction time (min)		
bile salts	celecoxib	nevirapine	flibanserin
pH 6.5 buffer control	5 ± 2	2 ± 1	5.4 ± 0.4
free bile salts			
SC	281 ± 40	15.6 ± 0.6	26 ± 12
SDC	>16 h	523 ± 9	0[b]
SCDC	103 ± 70	186 ± 6	0[b]
SLC	364 ± 39[a]	0[b]	623 ± 152[b]
SUDC	128 ± 16[a]	19 ± 10	30 ± 13
SHDC	>16 h[a]	577 ± 214	81 ± 16
glycine conjugated			
SGC	124 ± 54	158 ± 17	56 ± 15
SGDC	3.8 ± 0.4	21 ± 7	15.9 ± 0.6
SGCDC	19 ± 8	28 ± 2	11 ± 2
SGUDC	>16 h[a]	61 ± 32	66 ± 6
taurine conjugated			
STC	103 ± 35	30 ± 5	35 ± 7
STDC	3 ± 1	17 ± 2	8 ± 2
STCDC	>16 h	344 ± 66	386 ± 100

[a]Ionization led to greater extent of solubilization. [b]Insoluble compounds were formed.

nucleation. Thus, the inhibitory effects of bile salts appear to vary greatly depending on the structure of both the bile salt and the drug. Further mechanistic investigations into how molecular interactions affect crystallization are warranted.

Effect of Drug and Bile Salt Concentrations. To rule out the possibility of solubilization being the main factor for the prolonged nucleation induction, induction time measurements with different drug C/C_s ratios were performed by changing the concentration of the bile salt and the model compound. STC, the most commonly used bile salt in biorelevant media, was selected for these studies with celecoxib and nevirapine.

Various concentrations of celecoxib and nevirapine were evaluated with 0.1% STC in pH 6.5 buffer solutions, and their induction time was recorded as shown in Figures 2A and 3A. Similar trends were seen for both drugs. As drug concentration increases (higher supersaturation), the induction time decreases. The induction time of buffer controls is also shown in Figure 2A and 3A. It can be seen that STC extended the induction time of celecoxib and nevirapine at all concentrations tested relative to the buffer control.

The effect of STC concentration on induction times for celecoxib and nevirapine is shown in Figures 2B and 3B. The crystalline solubility values of celecoxib and nevirapine with different concentrations of STC are shown in Table 5. For celecoxib, the induction time increased as STC concentration increased. Increased STC concentration also promoted the solubilization of celecoxib (Table 5). Therefore, for celecoxib, delayed nucleation can be attributed to both solubility enhancement and increased nucleation inhibitor concentration. For nevirapine, no solubilization was observed at STC concentrations equal to or lower than 0.2% (Table 5). Therefore, solubilization was not responsible for the prolonged nucleation times for nevirapine at low STC concentrations. The induction time for nevirapine increased with increasing STC concentration from 0.1% to 0.4%, decreased as STC increased from 0.4% to 0.5%, and then increased again (Figure 3C). STC

DOI: 10.1021/acs.cgd.6b01470
Cryst. Growth Des. XXXX, XXX, XXX−XXX

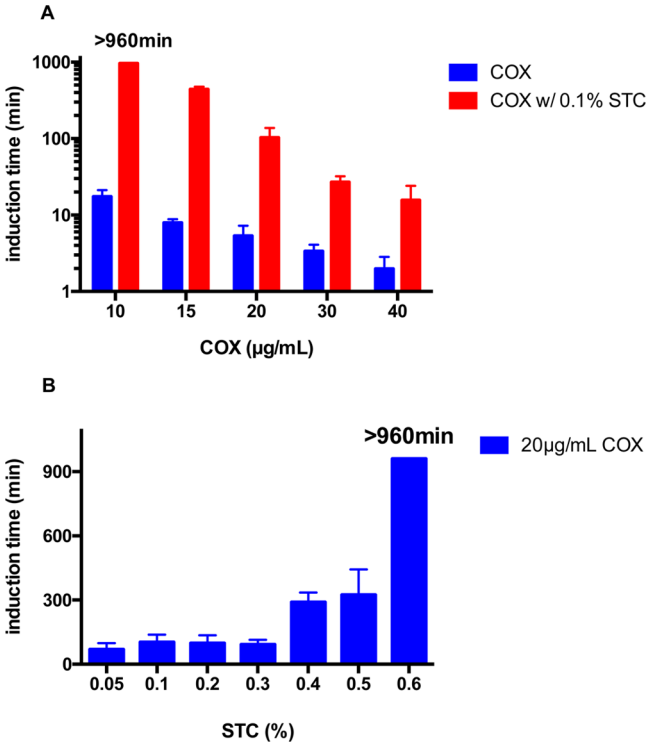

Figure 2. Nucleation induction time of celecoxib. (A) Effect of COX concentration on induction time with and without STC. (B) Effect of STC concentration on induction time with 20 μg/mL celecoxib.

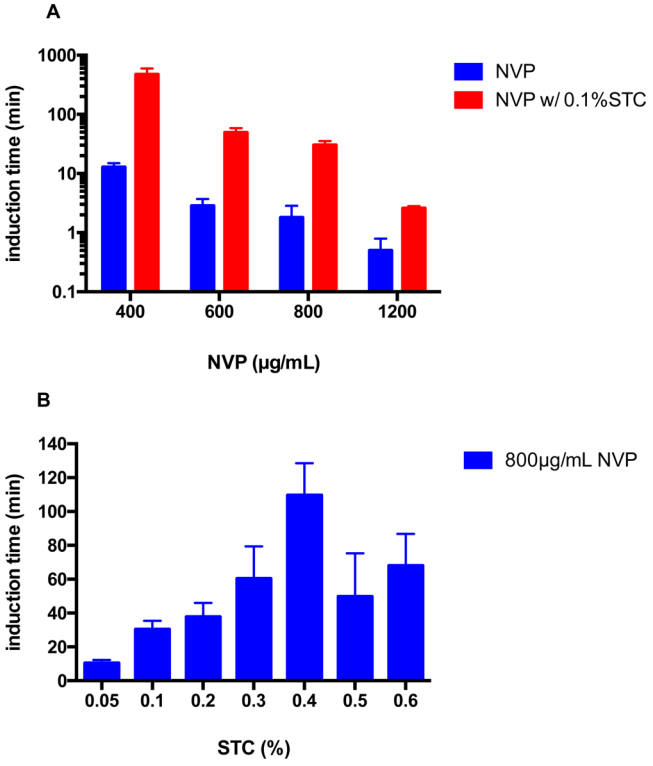

Figure 3. Nucleation induction time of nevirapine. (A) Effect of NVP concentration on induction time with and without STC. (B) Effect of STC concentration on induction time with 800 μg/mL NVP.

has been reported to possess stepwise aggregation behavior.[41] Therefore, changes in the aggregation behavior might lead to variations in nucleation inhibition properties as observed in nevirapine.

Table 5. Equilibrium Solubility Values of Celecoxib and Nevirapine with Various Amount of STC

	celecoxib		nevirapine	
STC content (%)	equilibrium solubility (μg/mL)	apparent supersaturation ratio	equilibrium solubility (μg/mL)	apparent supersaturation ratio
0	1.2 ± 0.1	13.6	105 ± 5	7.6
0.05	2.4 ± 0.6	8.5	102 ± 25	7.9
0.1	2.9 ± 0.2	6.8	101 ± 2	7.9
0.2	2.5 ± 0.1	8.2	104 ± 27	7.7
0.3	3.2 ± 0.5	6.3	112 ± 7	7.2
0.4	3.4 ± 0.2	5.9	125 ± 7	6.4
0.5	4.1 ± 0.4	4.3	124 ± 9	6.4
0.6	7.1 ± 0.9	2.9	134 ± 11	6.0

The CMCs of STC and SGC in the presence of celecoxib were measured and results are shown in Figure 4. It can be seen

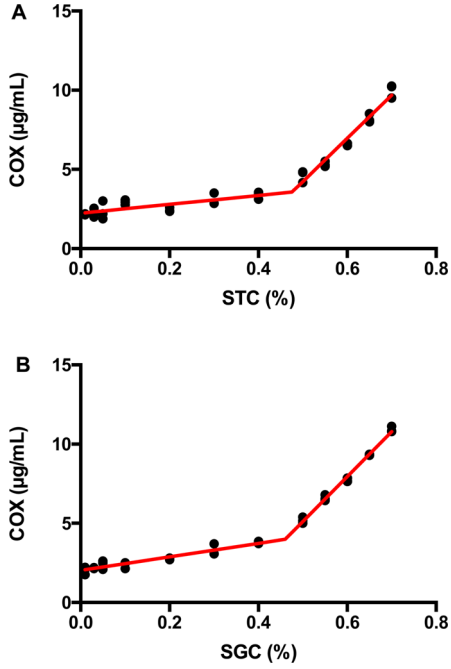

Figure 4. CMCs (aggregation numbers) of STC and SGC in the presence of celecoxib as determined by measuring crystalline solubility as a function of bile salt concentration. (A) STC. (B) SGC.

the bile salt concentration of 0.1% (w/v) used for the majority of the induction time measurements was well below the CMC of STC and SGC in the presence of celecoxib. However, at STC and SGC concentrations below their CMCs, the crystalline solubility of celecoxib increased slightly compared to that in the absence of bile salts (Tables 3 and 5, Figure 4).

Molecular Dynamic Simulations. Atomistic molecular dynamics was employed to explore the intermolecular interactions between selected bile salts and nevirapine at the molecular level. Pairs of molecules (dimers) were simulated in the presence of water for 100 ns. Subsequently, differences in the intermolecular interactions between systems with different bile salts were analyzed by measuring the minimum distance between molecules of the drug and bile salt, the total number of hydrogen bonds formed by these species, and values of the

DOI: 10.1021/acs.cgd.6b01470
Cryst. Growth Des. XXXX, XXX, XXX−XXX

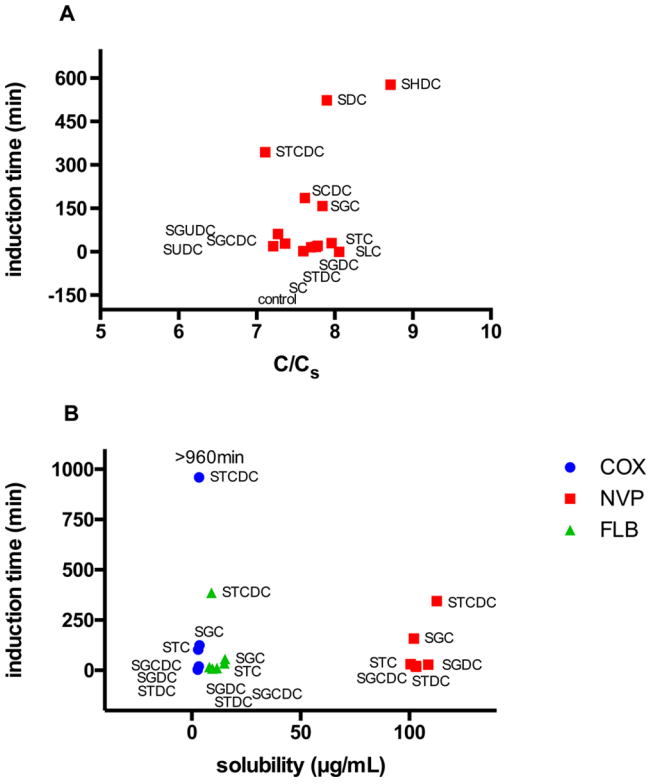

Figure 5. (A) Induction time vs supersaturation ratio for NVP and (B) induction time vs drug solubility in the presence of the six human bile salts.

interaction energies. Interaction energies in complexes of drug and other molecules are typically reported for the most stable conformation.[42−45] In contrast, we have explored diverse conformations in which the bile salt and the drug could be found in solution, and the propensity of these molecules to be in contact with each other. Therefore, the interaction energies reported herein are averages of multiple probable conformations. It should be noted that our goal in this work is not to simulate the nucleation process but to determine if MD simulations of small systems provide useful information for understanding differences in the inhibition of the crystallization of drug molecules.

Figure 6 shows a comparison between the interactions of two bile salts, SHDC and SC, and nevirapine, from MD trajectories containing one drug and one bile salt molecule. These two bile salts were chosen for simulations because SHDC is very effective at inhibiting nevirapine crystallization, while SC is ineffective. The histogram in Figure 6A shows the minimum distance between molecules of the bile salt and the drug during MD trajectories, which helps to determine the predisposition of the molecules to be in close contact. The minimum distances between drug and bile salt molecules range from 0.2 to 2.5 nm. It is clear that NVP and SHDC prefer to stay in close contact, with a high probability of being separated by only 0.2−0.3 nm, while NVP and SC are separated by 1.0−2.5 nm during approximately one-quarter of the trajectory.

Bile salts can interact with nevirapine by forming hydrogen bonds between the hydroxyl groups on the polar side of the bile salt or between carboxyl groups of bile salt with the nitrogen or the carbonyl group in nevirapine. The chemistry of the bile salt, i.e., the number and position of the hydroxyl groups, has a drastic impact on the total number of hydrogen bonds

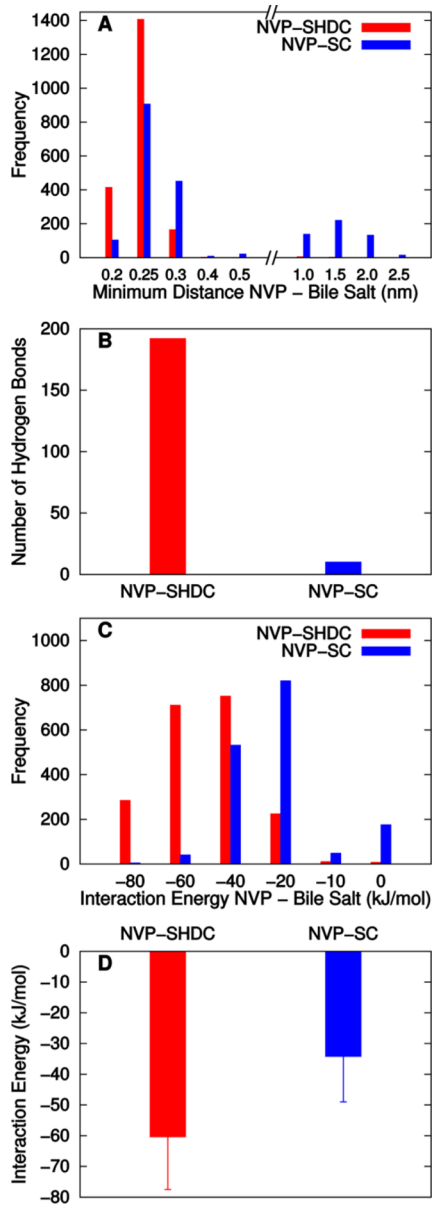

Figure 6. Comparison of intermolecular interactions between nevirapine and two bile salts molecules, SHDC and SC, based on 100 ns MD trajectories (2000 frames) including drug-bile salt dimers NVP-SHDC (red) and NVP-SC (blue). (A) Histogram showing the minimum distance distribution between bile salt and nevirapine during the trajectory. (B) The total number of intermolecular hydrogen bonds during the trajectory is plotted. (C) Histogram showing the interaction energy distribution between bile salt and nevirapine during the trajectory and (D) average interaction energy along the trajectory.

observed, as shown in Figure 6B. During the entire MD trajectories, the total count of hydrogen bonds in NVP-SHDC complex was 192, whereas only 10 hydrogen bonds were counted in the NVP-SC system.

The histogram in Figure 6C contains information about the distribution of interaction energies during the trajectory. As can be seen, NVP-SHDC complexes tend to possess stronger interactions, between −80 and −20 kJ/mol, whereas NVP-SC interactions are in the −40 and −20 kJ/mol range. Figure 6D summarizes the average interaction energy during the simulation, with values around −60 kJ/mol for SHDC and −30 kJ/mol for SC.

DOI: 10.1021/acs.cgd.6b01470
Cryst. Growth Des. XXXX, XXX, XXX−XXX

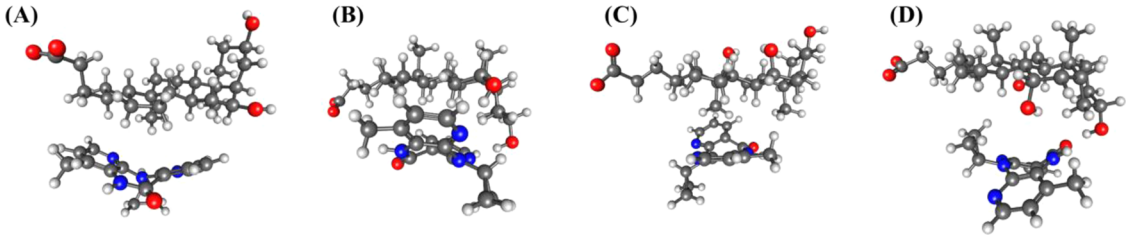

Figure 7. Representative dimer structures extracted from the MD trajectories of NVP−SHDC and NVP−SC dimers. (A) NVP−SHDC dimer interacting by the nonpolar face (B) NVP−SHDC dimer interacting via the polar face through hydrogen bonds (C) NVP−SC dimer interacting via the nonpolar face and (D) NVP−SC dimer interacting via its polar face.

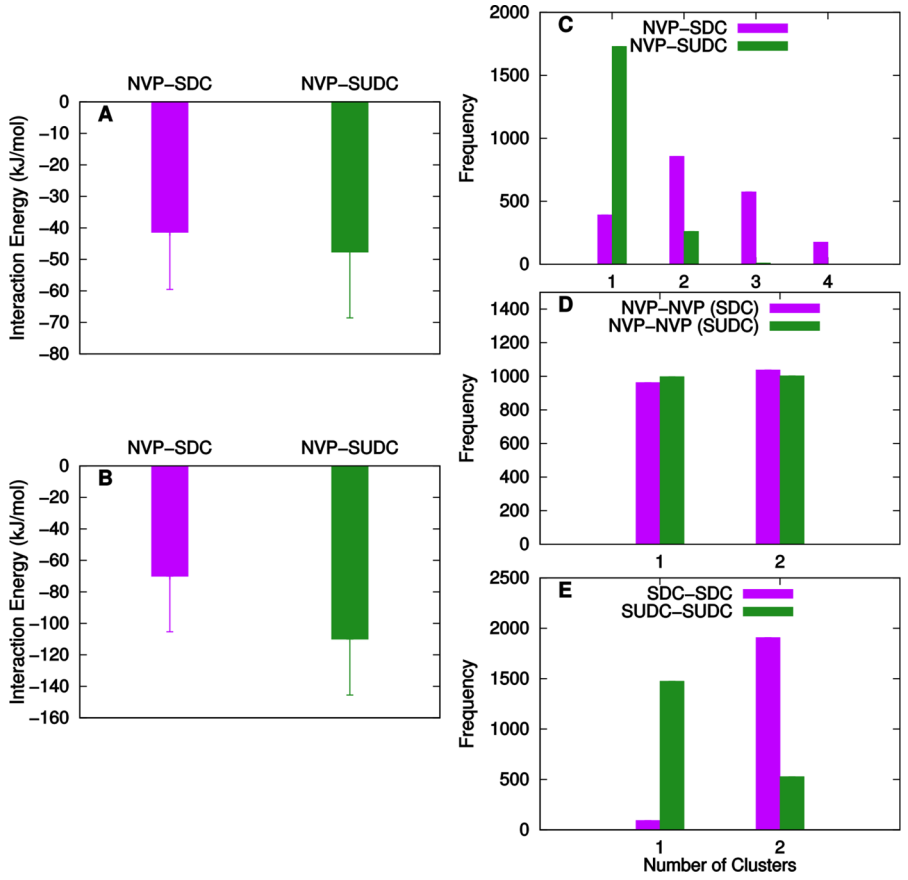

Figure 8. Comparison of intermolecular interactions between nevirapine and two bile salts molecules, SDC and SUDC. Information extracted from 100 ns MD trajectories (2000 frames) of (A) drug-bile salt dimers and (B, C, D, E) tetramers, NEV−SDC (magenta) and NEV−SUDC (green). Total interaction energy in NVP-bile salt (A) dimers and (B) tetramers. (C) The number of drug-bile salt clusters from the MD trajectories, where the numbers indicate: 1 (tetramer), 2 (two dimers), 3 (1 dimer and two molecules separated), 4 (noninteracting molecules). (D) The number of drug−drug clusters, and (E) the number of bile salt-bile salt clusters, where 1 shows that both molecules are interacting, while 2 reflects that the two molecules are separated.

Figure 7 shows representative conformations observed in MD trajectories of one drug and one bile salt molecule, in which nevirapine is involved in both polar (hydrogen bonding) and nonpolar (van der Waals) interactions with bile salts. When the drug interacts with the polar faces of the bile salt, NVP stays in closer contact with SHDC (Figure 7B) than with SC (Figure 7D). NVP−SHDC tend to form tightly arranged complexes, which may explain the predisposition of SHDC to form intermolecular hydrogen bonds during the trajectory.

Results from the MD simulations show that SHDC interacts with NVP for the majority of the trajectory, through van der Waals and hydrogen-bonded interactions. NVP−SC interactions are more dynamic, with sporadic interactions occurring throughout the trajectory, and mainly via van der Waals forces. These observations explain the more attractive interaction energies for NVP-SHDC than for NVP-SC and provide a perspective with regard to variations in crystallization inhibition by these two bile salts.

Similarly, the interaction patterns between two other bile salts, SDC and SUDC, and nevirapine were examined (Figure 8A). Although SDC is effective and SUDC is ineffective at inhibiting crystallization, MD simulations of one hydrated drug molecule and one bile salt resulted in similar interaction energies in heterodimers. Consequently, we extended MD simulations to include two bile salt and two drug molecules to establish the most probable interactions in these more complex

DOI: 10.1021/acs.cgd.6b01470
Cryst. Growth Des. XXXX, XXX, XXX−XXX

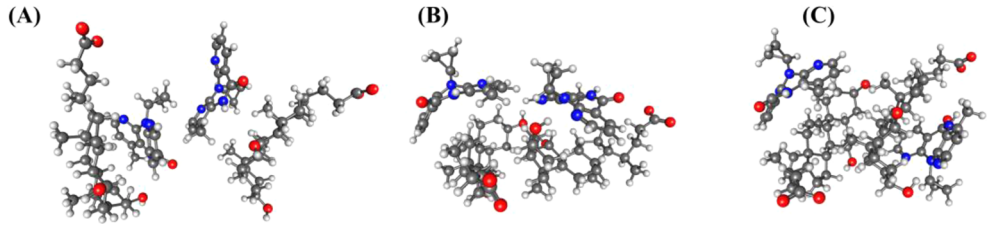

Figure 9. Representative structures of tetramers observed in MD simulations of two SUDC and two NVP molecules. (A) Drug molecules interacting in the center of the cluster, (B) bile salts and drug molecules interacting simultaneously, and (C) bile salts interacting in the center of the cluster.

systems. In other words, our goal was to determine if the drug molecules tend to interact with the bile salt molecules or with other drug molecules. Figure 8B shows average interaction energies in tetramers (four molecules: two of the drug and two of the bile salt), with more negative (attractive) values observed for NVP−SUDC than for NVP−SDC. This can be rationalized by the preferential formation of tetramer clusters in NVP−SUDC solutions, but mainly dimers and trimers in NVP−SDC systems, as demonstrated in Figure 8C. For example, NVP−SUDC tetramers are observed in 86% of the snapshots of the MD trajectory.

Figure 9 shows possible conformations of the NVP−SUDC tetramers. In some cases, the two drug molecules are closely interacting, and in others, SUDC−SUDC dimers are observed inside the cluster. Compared to dimers, additional interactions are allowed for in tetramers, and they contribute to a more negative (favorable) interaction energy for SUDC than for SDC. Therefore, simulations of systems containing several drug and bile salt molecules suggest that a more favorable interaction energy is not a general indication of a better bile salt system in terms of crystallization inhibitory ability.

Figure 8C,D reflects the numbers of NVP−NVP and bile salt−bile salt clusters during the trajectory. Nevirapine is interacting with itself approximately 50% of the time for both SUDC and SDC systems. In contrast, SUDC shows a preference for self-interaction, while SDC molecules tend to be separated. For example, SUDC−SUDC clusters are observed during 73% of the trajectory, whereas SDC−SDC clusters occur in only 5% of the trajectory. Accordingly, SUDC molecules tend to strongly self-interact as well as build up complexes with drug molecules.

In conclusion, our results show that the isolated use of interaction energies in drug−bile salt dimers is insufficient to explain why some bile salts are more effective crystallization inhibitors than others. Thus, it appears to be important to analyze intermolecular distances, hydrogen bonds, and cluster sizes, and to study larger systems to gather more consistent information.

DISCUSSION

Solubilization and Supersaturation. The role of supersaturation in improving the oral drug delivery of poorly water-soluble drugs is receiving increasing attention. Supersaturating dosage forms such as amorphous solid dispersions, where the drug is combined with a polymer to form a molecular level dispersion, are increasingly being used to improve the oral exposure of drugs.[46] Surfactants are commonly added to amorphous solid dispersion formulations or suspending media in order to increase the wettability, solubility, and in some cases, the release, of poorly water-soluble active pharmaceutical ingredients (APIs). However, the addition of surfactants can affect the supersaturation behavior and may promote crystallization.[47−49] Therefore, proper selection of the surfactant is vital to maintain the stability and performance attributes of amorphous solid dispersions. Furthermore, the impact of surfactants present in dissolution testing media needs to be carefully considered, in particular, if predictions about in vivo behavior are being made on the basis of these in vitro tests.

The impact of bile salts on the crystallization kinetics of supersaturated solutions is of particular interest since they are present in vivo (predominantly in the small intestine, but also at a lower concentration in the stomach) and are also frequently used in dissolution testing media. Hence their impact on the duration of supersaturation may be a key factor in determining the bioavailability of compounds that undergo supersaturation in vivo following oral delivery. This may be especially important for biopharmaceutical classification system (BCS) class 4 compounds, as the transit times are longer than those for class 2 compounds. On the basis of the results shown in Table 4, it is apparent that many of the bile salts evaluated retard the solution nucleation of celecoxib, nevirapine, and flibanserin, extending the longevity of the supersaturated solution. It was proposed in a recent study that the amphiphilicity of STC combined with a bulky hydrophobic group and a lack of flexibility contributes to its observed inhibitory impact.[49] This effect is in contrast to that observed for the more flexible surfactant, sodium dodecyl sulfate, which was found to promote the crystallization of several poorly water-soluble drugs.[15] However, in another study, a much higher concentration of STC than those used in this study (17 mM) was found to accelerate the nucleation of carbamazepine dihydrate from bulk aqueous solution.[47] In the same study, it was noted that STC inhibited the growth of carbamazepine dihydrate crystals along the *b* axis crystallographic direction. This was attributed to hydrogen bonding interactions between STC and the functional groups on the carbamazepine dihydrate crystal faces,[22] which interfered with the formation of a hydrogen-bonded chain of water and carboxamide dimers.[47]

Given that other bile salts have structural similarity to STC, the main purpose of this study was to compare nucleation induction times for multiple bile salts and attempt to explore potential relationships between properties such as solubilization capacity or bile salt structure, and the impact on nucleation. Hence a brief review of bile salt properties is warranted. Bile salts are well-known to form aggregates in solution, showing complex, stepwise aggregation. According to the widely accepted model developed by Small and co-workers, primary aggregates are formed at low bile salt concentrations by interaction between the hydrophobic, convex β-faces of the steroid ring of the bile salt molecules.[50] These aggregates are considered to have hydrophobic binding sites, and consequently hydrophobic molecules can interact with the aggregates.[51−53] These interactions give rise to the well-

DOI: 10.1021/acs.cgd.6b01470
Cryst. Growth Des. XXXX, XXX, XXX−XXX

known solubilization of drugs by bile salt micelles whereby hydrophobic molecules are incorporated into the micelles.[40,54] As the bile salt concentration increases, primary aggregates form secondary aggregates through hydrogen bonding interactions. The aggregation numbers for the primary aggregates are around 2−10 molecules, with this number increasing as secondary aggregates form.[13] The CMC values (aggregation numbers) for bile salts are highly dependent on the method used for determination as well as the experimental conditions.[55] The trihydroxy bile salts such as STC are more water-soluble and have higher CMCs, typically in the range of 10−15 mM, while the CMC values of the less soluble dihydroxy bile salts are normally less than 5 mM. The experimental CMCs of STC and SGC in the presence of celecoxib were 0.48% and 0.46% (w/v), respectively, as determined based on their ability to enhance the crystalline solubility (Figure 4). The CMCs of all bile salts tested in the presence of nevirapine can be inferred to be above 0.1% (w/v) as the crystalline solubility of nevirapine was not affected at this bile salt level (Table 3). Literature CMC values for the bile salts used in this study are compiled in Table 1. Most of the reported CMC values for different bile salts are above 2 mM,[56] higher than the concentration of 1.86 mM (0.1% w/w) used in this study. Therefore, the majority of the bile salt in the solutions evaluated herein can be considered to be present at concentrations lower than the CMC and therefore present as monomers or low order aggregates.

From classical nucleation theory, it is well-known that nucleation rate is highly dependent on the extent of supersaturation in the system. When evaluating nucleation kinetics and the impact of additives, it is important to consider the level of supersaturation in the solution.

The supersaturation is the excess free drug concentration over the free drug concentration of a saturated solution and is given by following equation:

$$S = \frac{a}{a_{s*}} = \frac{C\gamma}{C_{s*}\gamma_{s*}} \tag{3}$$

where a is the solute activity, C is the concentration, and γ is the activity coefficient. The subscript s* indicates the property at saturation, where the solute in solution is in equilibrium with the crystal.[57] It is commonly assumed that $\frac{\gamma}{\gamma_s}$ is 1 and hence eq 3 reduces to eq 1.

It has been demonstrated that solubilizing additives (those that increase the solubility of the crystalline drug) can reduce the supersaturation, even if the total concentration of drug in solution remains constant;[26] this is also expected based on eq 1. Therefore, one reason for the increased induction times observed in this study in the presence of the bile salts might be due to a reduction in supersaturation due to solubilization of the crystalline form of the drug. Table 3 shows that the crystal solubility is only increased by a small amount in the presence of 0.1% bile salt (compared to the typical increases in solubility observed in the presence of bile salts that are above their CMC).[40,58] This is particularly true for nevirapine, where there is essentially no change in the crystal solubility. This weakly basic compound, with pK_a of 2.8, is also essentially un-ionized for all pH conditions evaluated in this study. Assuming that C/C_s provides a good approximation of the supersaturation, it can be seen from Figure 5A that the induction time measurements do not correlate with S'; S' is nearly constant across the different experiments, while the induction times vary considerably. In fact, the system with the highest supersaturation based on the C/C_s ratio has the longest induction time.

Given the importance of supersaturation in determining the nucleation rate, combined with previous reports that eq 1 does not always give reasonable estimates of S in the presence of surfactants,[26] flux studies were used to further investigate supersaturation in select systems of interest. As shown by eq 3, mass flow rates are directly proportional to solute activity and hence also to supersaturation given that the activity of the crystal is a constant. Table 6 shows that, within experimental error, the mass flow rates are identical for a given concentration of drug in the presence or absence of 0.1% STC or SGC. Hence, we can confirm that induction times for celecoxib and nevirapine was considerably extended when tested at the same crystallization driving force (i.e., supersaturation). These observations suggest that solubilization, with a consequent reduction in supersaturation, can be eliminated as the mechanism underlying the prolonged induction times for bile salt at a concentration level of 0.1%.

Table 6. Mass Flow and Crystalline Solubility of COX and NVP in the Presence and Absence of Bile Salts

	mass flow (μg/min)		crystalline solubility (μg/mL)	
additive	COX	NVP	COX	NVP
no additive	0.44 ± 0.07	20.9 ± 2.9	1.2 ± 0.1	108 ± 5
HPMCAS MF (5 μg/mL)	0.44 ± 0.02	22.6 ± 1.7	2.4 ± 0.1	126 ± 1
STC 0.1% (w/v)	0.46 ± 0.04	23.4 ± 2.8	2.9 ± 0.2	102 ± 1
SGC 0.1% (w/v)	0.41 ± 0.07	21.0 ± 3.6	2.4 ± 0.2	101 ± 2

Hydrophobicity. In order to gain some insights into the structural features of bile salts that may be important in affecting their crystallization inhibition ability, a comparison was made between bile salts with different structures. The molecular structures of the bile salts used in this study are shown in Table 1. Their structures differ depending on the presence or absence of hydroxyl groups as well as their orientation at the R2, R3, and R4 positions on the steroid ring. They can be further categorized into three groups based on the R5 group: free bile salts (O−), glycine conjugated ($NHCH_2COO-$), and taurine conjugated ($NHCH_2\ CH_2SO_3$-) bile salts. The physicochemical properties of different bile salt are listed in Table A in the Supporting Information. The taurine conjugates tend to have lower pK_a and log P'_A values, followed by glycine conjugates, and then free bile acids.[59] From the results summarized in Table 4, it appears that the free bile salts, as a group, tend to be better at prolonging induction times relative to the more hydrophilic conjugated bile salts.

The induction times of celecoxib, nevirapine, and flibanserin in the presence of bile salts with available Log P'_A values are plotted in Figure 10 (excluding systems undergoing ionization or forming insoluble particles), where the data are arranged left to right in order of decreasing bile salt Log P'_A. For all three model compounds, the nucleation inhibition ability of free bile salts (blue columns) generally increased with increasing log P'_A values; while for the glycine conjugated bile salts (red columns), induction times increased with decreasing log P'_A values. For taurine conjugated bile salts, only the log P'_A of STC is available and thus no trends are apparent. Studies on the binding of hydrophobic molecules with bile salt aggregates

DOI: 10.1021/acs.cgd.6b01470
Cryst. Growth Des. XXXX, XXX, XXX−XXX

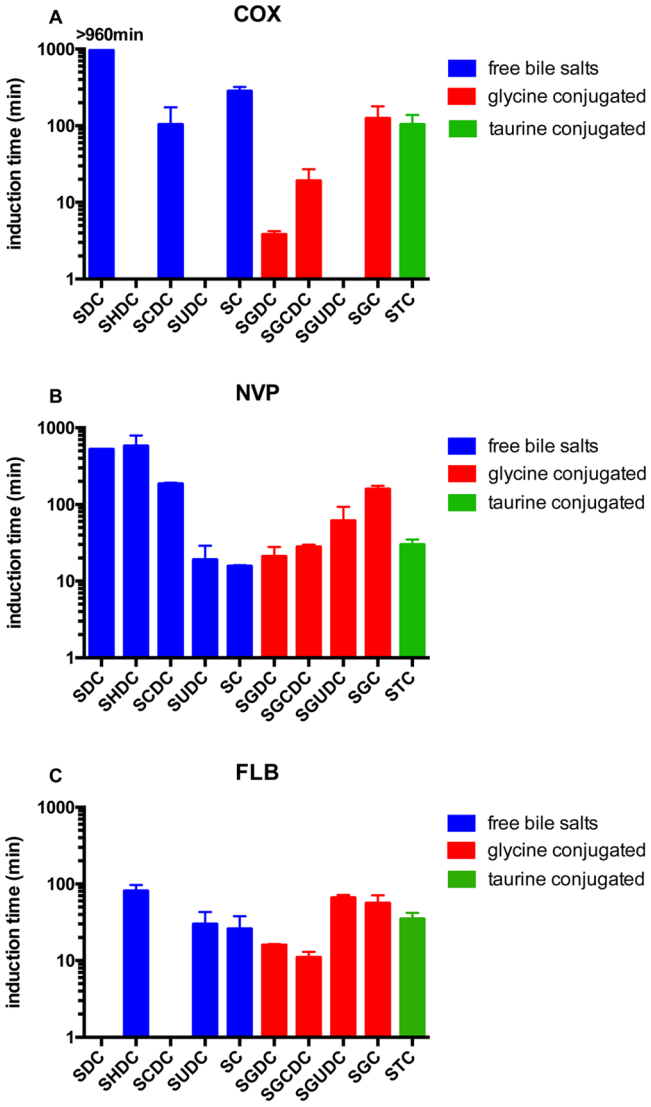

Figure 10. Induction times for celecoxib, nevirapine, and flibanserin in the presence of certain bile salts. From left to right: decreasing log P'_A values (see Table 1).

suggest that both hydrophobic interactions and hydrogen bonding with the bile salt headgroup are potentially important, but vary with both bile salt and guest molecule chemistry.[51] The MD simulations carried out herein indicate that the unconjugated bile salts interact with nevirapine via both hydrogen bonding and van der Waals interactions, with the extent of hydrogen bonding varying with bile salt chemistry (Figure 6). The observations summarized in Figure 10 suggest that, for the unconjugated bile salts, increased bile salt hydrophobicity, as inferred from log P'_A values, may lead to enhanced interactions with the drug or drug clusters which delay nucleation. However, average interaction energies for selected nevirapine-bile salt dimers, calculated from MD simulations, which encompass both hydrogen bonding and van der Waals interactions, do not correlate with nucleation inhibition in all instances. In the case of the glycine conjugated bile salts, the opposite trend may indicate that drug−bile salt hydrogen bonding interactions with the glycine headgroup also play an important role.

Only considering drug−bile salt dimer interactions provides an incomplete picture of factors likely to be important in inhibiting nucleation. Using molecular simulations, Anwar and colleagues studied the impact of additives on nucleation using a highly simplified system.[60] They found that the ability of additives to inhibit nucleation depended on the affinity of the additive for the crystallizing solute relative to the self-affinity and solvent affinity, as well as the additive size. Thus, additives with a high affinity for the solute were able to inhibit nucleation via incorporation into the nucleus and disruption of packing, whereas more amphiphilic additives were only able to delay nucleation via interactions at the surface of the nucleus. Given their surfactant-like properties, bile salts are likely to interact with the surface of the emerging nucleus, delaying rather than completely inhibiting nucleation, as observed in this study.

On the basis of the molecular structure of bile salts, the affinity for the drug can be expected to depend both on hydrogen bonding and van der Waals interactions. From MD simulations, both of these interactions were found to be important in determining the interaction energy. However, based on the simulations of Anwar et al.,[60] discussed above, the tendency of bile salt molecules to self-interact, as well as the structure of bile salt-drug aggregates are also likely to be important. While the average binary interaction energies between nevirapine and SHDC and SC correlate with their good and relatively poor nucleation inhibition respectively, these values fail to differentiate SUDC (poor inhibitor) and SDC (good inhibitor). SUDC however, shows a different pattern of behavior from SDC in that it tends to self-aggregate, even in the presence of nevirapine molecules, while SDC tends to remain monomeric (Figure 8E). This may indicate a lower tendency to interact with a nevirapine nucleus. Clearly more sophisticated modeling of the nucleation process is required in order to gain additional insight into the subtle differences between bile salt−drug interactions that lead to the observed differences in nucleation inhibitory ability.

Biorelevance. It is of interest to compare the inhibitory ability of the bile salts that are abundant in human bile. On the basis of studies of human intestinal fluids, conjugated bile salts dominate bile salt profiles with glycine conjugated salts being more prevalent than the taurine conjugated salts.[61−64] The percentage abundance of the six most prevalent human bile salts that we studied is listed in Table 1.[65] This may vary from person to person, however.[62] The induction time data for these six bile salts is summarized in Figure 5B. Here it is readily apparent that, although several of these bile salts have an inhibitory impact on crystallization, STCDC possessed the highest nucleation inhibitory effect. SGC, which is one of the two most abundant bile salts in human bile (on average, approximately 30% of bile is comprised of SGC based on literature studies of human intestinal fluid (HIF) composition[61,65]) appears to be the second most effective inhibitor for the three compounds. In agreement with previous studies,[15,49] STC is also quite effective in prolonging the induction times. More variability in induction time effects and compound dependence is seen for the remaining bile salts. To better understand the crystallization inhibition properties of human bile, we combined the six most prevalent human bile salts to mimic human bile composition (Table 1) and conducted induction time measurements for celecoxib at a total bile salt concentration of 0.1%. The induction time of celecoxib was 210 ± 21 min. This is longer than that seen for the 0.1% STC solution, where the induction time for celecoxib at the same drug concentration was approximately 100 min (Table 4). This observation suggests that crystallization kinetics in vivo may not

DOI: 10.1021/acs.cgd.6b01470
Cryst. Growth Des. XXXX, XXX, XXX−XXX

be adequately predicted by experiments in commonly used simulated media. However, our system is also a simplified one, and the presence additional components such as lecithin may further alter both solubility and crystallization kinetics. This is clearly an area for future study.

The concentration dependence of the nucleation inhibitory effect was evaluated with STC (Figures 2 and 3) and the concentration ranges of STC used in biorelevant media are shown in Table 7. During the development of biorelevant media, STC was selected to help simulate the solubilization power of human GI fluids.[66] However, its impact on maintaining supersaturation has not been considered. Given the increase in the number of supersaturating formulations being developed and evaluated, it is of interest to consider STC in this context. The bile salt concentration used in this study to compare the different bile salts is slightly lower than the concentration of STC in FaSSIF and the total concentration of bile salts found in the human GI tract in the fasted state (Table 7). If the concentration of STC is increased (Figures 2 and 3), then the induction times appear to increase, although it should be recognized that this may be due, in part, to solubilization, since the crystalline solubility increases with increasing bile salt concentration (Table 5), reducing the supersaturation and the driving force for nucleation. Given the observed concentration dependence, the nucleation inhibition effect may be more pronounced in vivo, especially considering the difference in hydrodynamics between our vigorously stirred lab experiment and the GI environment. Furthermore, one of the most in vivo abundant bile salts, SGC, was found to be more effective at inhibiting nucleation than STC for all three compounds studied, which might also lead to different observations in vivo. Therefore, attention should be paid to bile salt selection for biorelevant dissolution media when evaluating supersaturating dosage forms, as they are not equivalent with regard to their crystallization inhibitory properties.

Table 7. Bile Salt Concentration in Human Gastrointestinal Track and Biorelevant Dissolution Media

	STC (mg/mL)	bile salts (mg/mL)
fasted state simulated intestinal fluid (FaSSIF)	1.613 (3 mM)	
fed state simulated intestinal fluid (FeSSIF)	8.065 (15 mM)	
fasted state simulated gastric fluid (FaSSGF)	0.043 (0.08 mM)	
human jejunum[20]		0.60−2.85 (1.52−5.30 mM)
human duodenum[20]		0.56−3.17 (1.40−5.90 mM)
this study	1 (1.86 mM)	1 (1.86−2.51 mM)

CONCLUSIONS

The impact of 13 bile salts on the solution induction times of three drugs, celecoxib, nevirapine, and flibanserin, was tested. Most bile salts inhibited solution nucleation of these fast crystallizing compounds to some extent. However, their inhibition effects varied depending on the structure of both the bile salt and the drug. For free bile salts, better nucleation inhibition properties were observed for bile salts with higher hydrophobicity; for glycine conjugated bile salts, the opposite trend was seen. MD simulations showed complex interactions between nevirapine and bile salts, making it challenging to deconvolute the molecular origin of the nucleation inhibition effects. On the basis of these findings, the presence of bile salts in the human GI tract could delay the crystallization of supersaturated solutions of poorly soluble drug candidates. Attention should be also paid to bile salt selection for biorelevant dissolution media, as they are not interchangeable in the context of crystallization inhibitory ability. Finally, evaluation of small molecule crystallization inhibitors is of general importance in the context of supersaturating dosage forms.

ASSOCIATED CONTENT

Supporting Information

The Supporting Information is available free of charge on the ACS Publications website at DOI: 10.1021/acs.cgd.6b01470.

Details about the physicochemical properties of the bile salts (PDF)

AUTHOR INFORMATION

Corresponding Author

*Phone: (765) 496-6614. Fax: (765) 494-6545. E-mail: lstaylor@purdue.edu.

Notes

The authors declare no competing financial interest.

ACKNOWLEDGMENTS

This study was supported by Merck & Co., Inc. We thank the National Science Foundation for funding this work through Award Number DMR-1309218 (L.S.T. and L.M.). L.V.S. and C.H.B. acknowledge funding from the NSF Grant CHE-1465154. This research was supported in part by a Graduate Student Fellowship Award from the American Association of Pharmaceutical Scientists to L.M. Wei Xu, Amitava Mitra, Patrick Marsac, and Craig McKelvey are thanked for helpful discussions. This research was supported in part through computational resources provided by Information Technology at Purdue University.

ABBREVIATIONS

API, active pharmaceutical ingredients; COX, celecoxib; FaSSIF, fasted state simulated intestinal fluid; FaSSGF, fasted state simulated gastric fluid; FeSSIF, fed state simulated intestinal fluid; FLB, flibanserin; HIF, human intestinal fluid; NVP, nevirapine; SC, sodium cholate; SDC, sodium deoxycholate; SCDC, sodium chenodeoxycholate; SLC, sodium lithocholate; SUDC, sodium ursodeoxycholate; SHDC, sodium hyodeoxycholate; SGC, sodium glycocholate; SGDC, sodium glycodeoxycholate; SGCDC, sodium glycochenodeoxycholate; SGUDC, sodium glycoursodeoxycholate; STC, sodium taurocholate; STCDC, sodium taurochenodeoxycholate; STDC, sodium taurodeoxycholate

REFERENCES

(1) Amidon, G.; Lennernäs, H.; Shah, V.; Crison, J. A Theoretical Basis for a Biopharmaceutic Drug Classification: The Correlation of in Vitro Drug Product Dissolution and in Vivo Bioavailability. *Pharm. Res.* **1995**, *12* (3), 413−420.

(2) Rangel-Yagui, C. O.; Pessoa, A., Jr; Tavares, L. C. Micellar solubilization of drugs. *J. Pharm. Pharm. Sci.* **2005**, *8* (2), 147−163.

(3) Loftsson, T.; Duchêne, D. Cyclodextrins and their pharmaceutical applications. *Int. J. Pharm.* **2007**, *329* (1−2), 1−11.

DOI: 10.1021/acs.cgd.6b01470
Cryst. Growth Des. XXXX, XXX, XXX−XXX

(4) Strickley, R. G. Solubilizing excipients in oral and injectable formulations. *Pharm. Res.* **2004**, *21* (2), 201−230.
(5) Shegokar, R.; Müller, R. H. Nanocrystals: Industrially feasible multifunctional formulation technology for poorly soluble actives. *Int. J. Pharm.* **2010**, *399* (1−2), 129−139.
(6) Kwong, A. D.; Kauffman, R. S.; Hurter, P.; Mueller, P. Discovery and development of telaprevir: an NS3−4A protease inhibitor for treating genotype 1 chronic hepatitis C virus. *Nat. Biotechnol.* **2011**, *29* (11), 993−1003.
(7) di Cagno, M.; Luppi, B. Drug "supersaturation" states induced by polymeric micelles and liposomes: A mechanistic investigation into permeability enhancements. *Eur. J. Pharm. Sci.* **2013**, *48* (4−5), 775−780.
(8) Katneni, K.; Charman, S. A.; Porter, C. J. H. Permeability assessment of poorly water-soluble compounds under solubilizing conditions: The reciprocal permeability approach. *J. Pharm. Sci.* **2006**, *95* (10), 2170−2185.
(9) Raghavan, S. L.; Trividic, A.; Davis, A. F.; Hadgraft, J. Crystallization of hydrocortisone acetate: influence of polymers. *Int. J. Pharm.* **2001**, *212* (2), 213−221.
(10) Ilevbare, G. A.; Liu, H.; Edgar, K. J.; Taylor, L. S. Maintaining Supersaturation in Aqueous Drug Solutions: Impact of Different Polymers on Induction Times. *Cryst. Growth Des.* **2013**, *13* (2), 740−751.
(11) Warren, D. B.; Benameur, H.; Porter, C. J. H.; Pouton, C. W. Using polymeric precipitation inhibitors to improve the absorption of poorly water-soluble drugs: A mechanistic basis for utility. *J. Drug Targeting* **2010**, *18* (10), 704−731.
(12) Mosquera-Giraldo, L. I.; Borca, C. H.; Meng, X.; Edgar, K. J.; Slipchenko, L. V.; Taylor, L. S. Mechanistic Design of Chemically Diverse Polymers with Applications in Oral Drug Delivery. *Biomacromolecules* **2016**, DOI: 10.1021/acs.biomac.6b01156.
(13) Mukhopadhyay, S.; Maitra, U. Chemistry and biology of bile acids. *Curr. Sci. India* **2004**, *87* (12), 1666−1683.
(14) Jantratid, E.; Janssen, N.; Reppas, C.; Dressman, J. Dissolution Media Simulating Conditions in the Proximal Human Gastrointestinal Tract: An Update. *Pharm. Res.* **2008**, *25* (7), 1663−1676.
(15) Chen, J.; Mosquera-Giraldo, L. I.; Ormes, J. D.; Higgins, J. D.; Taylor, L. S. Bile salts as crystallization inhibitors of supersaturated solutions of poorly water-soluble compounds. *Cryst. Growth Des.* **2015**, *15*, 2593−2597.
(16) Carlert, S.; Pålsson, A.; Hanisch, G.; von Corswant, C.; Nilsson, C.; Lindfors, L.; Lennernäs, H.; Abrahamsson, B. Predicting Intestinal Precipitation—A Case Example for a Basic BCS Class II Drug. *Pharm. Res.* **2010**, *27* (10), 2119−2130.
(17) Ferro, L. J.; Miyake, P. S.*Polymorphic Crystalline Forms of Celecoxib*. US patent. US7476744 B2, 2009.
(18) Liebenberg, W.; Stieger, N.*Nevirapine polymorph.* European patent. EP 2499141B, 2011.
(19) Bombarda, C.; Dubini, E.; Ezhaya, A. *Stable Polymorph of Flibanserin, Technical Process for Its Preparation and the Use Thereof for Preparing Medicament* European patent. EP 1518858 A1, 2005
(20) Fuchs, A.; Dressman, J. B. Composition and Physicochemical Properties of Fasted-State Human Duodenal and Jejunal Fluid: A Critical Evaluation of the Available Data. *J. Pharm. Sci.* **2014**, *103* (11), 3398−3411.
(21) Mullin, J. W. *Crystallization*. 4th ed.; Butterworth-Heinemann: Oxford, 2001.
(22) Cerdeira, M.; Candal, R. J.; Herrera, M. L. Analytical Techniques for Nucleation Studies in Lipids: Advantages and Disadvantages. *J. Food Sci.* **2004**, *69* (9), R185−R191.
(23) Kuldipkumar, A.; Kwon, G. S.; Zhang, G. G. Z. Determining the Growth Mechanism of Tolazamide by Induction Time Measurement. *Cryst. Growth Des.* **2007**, *7* (2), 234−242.
(24) Alonzo, D. E.; Raina, S.; Zhou, D.; Gao, Y.; Zhang, G. G. Z.; Taylor, L. S. Characterizing the Impact of Hydroxypropylmethyl Cellulose on the Growth and Nucleation Kinetics of Felodipine from Supersaturated Solutions. *Cryst. Growth Des.* **2012**, *12* (3), 1538−1547.
(25) Ilevbare, G. A.; Taylor, L. S. Liquid−Liquid Phase Separation in Highly Supersaturated Aqueous Solutions of Poorly Water-Soluble Drugs: Implications for Solubility Enhancing Formulations. *Cryst. Growth Des.* **2013**, *13* (4), 1497−1509.
(26) Raina, S.; Zhang, G. Z.; Alonzo, D.; Wu, J.; Zhu, D.; Catron, N.; Gao, Y.; Taylor, L. Impact of solubilizing additives on supersaturation and membrane transport of drugs. *Pharm. Res.* **2015**, *32* (10), 3350−3364.
(27) Van Der Spoel, D.; Lindahl, E.; Hess, B.; Groenhof, G.; Mark, A. E.; Berendsen, H. J. C. GROMACS: Fast, flexible, and free. *J. Comput. Chem.* **2005**, *26* (16), 1701−1718.
(28) Hess, B.; Kutzner, C.; van der Spoel, D.; Lindahl, E. GROMACS 4: Algorithms for Highly Efficient, Load-Balanced, and Scalable Molecular Simulation. *J. Chem. Theory Comput.* **2008**, *4* (3), 435−447.
(29) Brooks, B. R.; Bruccoleri, R. E.; Olafson, B. D.; States, D. J.; Swaminathan, S.; Karplus, M. CHARMM: A program for macromolecular energy, minimization, and dynamics calculations. *J. Comput. Chem.* **1983**, *4* (2), 187−217.
(30) MacKerell, A. D.; Banavali, N.; Foloppe, N. Development and current status of the CHARMM force field for nucleic acids. *Biopolymers* **2000**, *56* (4), 257−265.
(31) Stieger, N.; Liebenberg, W.; Wessels, J. C.; Samsodien, H.; Caira, M. R. Channel inclusion of primary alcohols in isostructural solvates of the antiretroviral nevirapine: an X-ray and thermal analysis study. *Struct. Chem.* **2010**, *21* (4), 771−777.
(32) Cobbledick, R. E.; Einstein, F. W. B. The structure of sodium 3[alpha],7[alpha],12[alpha]-trihydroxy-5[beta]-cholan-24-oate monohydrate (sodium cholate monohydrate). *Acta Crystallogr., Sect. B: Struct. Crystallogr. Cryst. Chem.* **1980**, *36* (2), 287−292.
(33) Gilbert, A. T. B. IQmol molecular viewer. Available at http://iqmol.org. (Accessed October 2012).
(34) Shao, Y.; Gan, Z.; Epifanovsky, E.; Gilbert, A. T. B.; Wormit, M.; Kussmann, J.; Lange, A. W.; Behn, A.; Deng, J.; Feng, X.; Ghosh, D.; Goldey, M.; Horn, P. R.; Jacobson, L. D.; Kaliman, I.; Khaliullin, R. Z.; Kuś, T.; Landau, A.; Liu, J.; Proynov, E. I.; Rhee, Y. M.; Richard, R. M.; Rohrdanz, M. A.; Steele, R. P.; Sundstrom, E. J.; Woodcock, H. L.; Zimmerman, P. M.; Zuev, D.; Albrecht, B.; Alguire, E.; Austin, B.; Beran, G. J. O.; Bernard, Y. A.; Berquist, E.; Brandhorst, K.; Bravaya, K. B.; Brown, S. T.; Casanova, D.; Chang, C.-M.; Chen, Y.; Chien, S. H.; Closser, K. D.; Crittenden, D. L.; Diedenhofen, M.; DiStasio, R. A.; Do, H.; Dutoi, A. D.; Edgar, R. G.; Fatehi, S.; Fusti-Molnar, L.; Ghysels, A.; Golubeva-Zadorozhnaya, A.; Gomes, J.; Hanson-Heine, M. W. D.; Harbach, P. H. P.; Hauser, A. W.; Hohenstein, E. G.; Holden, Z. C.; Jagau, T.-C.; Ji, H.; Kaduk, B.; Khistyaev, K.; Kim, J.; Kim, J.; King, R. A.; Klunzinger, P.; Kosenkov, D.; Kowalczyk, T.; Krauter, C. M.; Lao, K. U.; Laurent, A. D.; Lawler, K. V.; Levchenko, S. V.; Lin, C. Y.; Liu, F.; Livshits, E.; Lochan, R. C.; Luenser, A.; Manohar, P.; Manzer, S. F.; Mao, S.-P.; Mardirossian, N.; Marenich, A. V.; Maurer, S. A.; Mayhall, N. J.; Neuscamman, E.; Oana, C. M.; Olivares-Amaya, R.; O'Neill, D. P.; Parkhill, J. A.; Perrine, T. M.; Peverati, R.; Prociuk, A.; Rehn, D. R.; Rosta, E.; Russ, N. J.; Sharada, S. M.; Sharma, S.; Small, D. W.; Sodt, A.; Stein, T.; Stück, D.; Su, Y.-C.; Thom, A. J. W.; Tsuchimochi, T.; Vanovschi, V.; Vogt, L.; Vydrov, O.; Wang, T.; Watson, M. A.; Wenzel, J.; White, A.; Williams, C. F.; Yang, J.; Yeganeh, S.; Yost, S. R.; You, Z.-Q.; Zhang, I. Y.; Zhang, X.; Zhao, Y.; Brooks, B. R.; Chan, G. K. L.; Chipman, D. M.; Cramer, C. J.; Goddard, W. A.; Gordon, M. S.; Hehre, W. J.; Klamt, A.; Schaefer, H. F.; Schmidt, M. W.; Sherrill, C. D.; Truhlar, D. G.; Warshel, A.; Xu, X.; Aspuru-Guzik, A.; Baer, R.; Bell, A. T.; Besley, N. A.; Chai, J.-D.; Dreuw, A.; Dunietz, B. D.; Furlani, T. R.; Gwaltney, S. R.; Hsu, C.-P.; Jung, Y.; Kong, J.; Lambrecht, D. S.; Liang, W.; Ochsenfeld, C.; Rassolov, V. A.; Slipchenko, L. V.; Subotnik, J. E.; Van Voorhis, T.; Herbert, J. M.; Krylov, A. I.; Gill, P. M. W.; Head-Gordon, M. Advances in molecular quantum chemistry contained in the Q-Chem 4 program package. *Mol. Phys.* **2015**, *113* (2), 184−215.
(35) Zoete, V.; Cuendet, M. A.; Grosdidier, A.; Michielin, O. SwissParam: A fast force field generation tool for small organic molecules. *J. Comput. Chem.* **2011**, *32* (11), 2359−2368.

DOI: 10.1021/acs.cgd.6b01470
Cryst. Growth Des. XXXX, XXX, XXX−XXX

(36) Humphrey, W.; Dalke, A.; Schulten, K. VMD: Visual molecular dynamics. *J. Mol. Graphics* **1996**, *14* (1), 33−38.
(37) Subramanian, N.; Ray, S.; Ghosal, S. K.; Bhadra, R.; Moulik, S. P. Formulation Design of Self-Microemulsifying Drug Delivery Systems for Improved Oral Bioavailability of Celecoxib. *Biol. Pharm. Bull.* **2004**, *27* (12), 1993−1999.
(38) Cheeseman, S. H.; Hattox, S. E.; McLaughlin, M. M.; Koup, R. A.; Andrews, C.; Bova, C. A.; Pav, J. W.; Roy, T.; Sullivan, J. L.; Keirns, J. J. Pharmacokinetics of nevirapine: initial single-rising-dose study in humans. *Antimicrob. Agents Chemother.* **1993**, *37* (2), 178−182.
(39) Box, K. Private communication, 2014.
(40) Wiedmann, T. S.; Kamel, L. Examination of the solubilization of drugs by bile salt micelles. *J. Pharm. Sci.* **2002**, *91* (8), 1743−1764.
(41) O'Connor, C. J.; Ch'ng, B. T.; Wallace, R. G. Studies in bile salt solutions: 1. Surface tension evidence for a stepwise aggregation model. *J. Colloid Interface Sci.* **1983**, *95* (2), 410−419.
(42) Karavas, E.; Georgarakis, E.; Sigalas, M. P.; Avgoustakis, K.; Bikiaris, D. Investigation of the release mechanism of a sparingly water-soluble drug from solid dispersions in hydrophilic carriers based on physical state of drug, particle size distribution and drug−polymer interactions. *Eur. J. Pharm. Biopharm.* **2007**, *66* (3), 334−347.
(43) Lima, Á. A. N.; Soares-Sobrinho, J. L.; Silva, J. L.; Corrêa-Júnior, R. A. C.; Lyra, M. A. M.; Santos, F. L. A.; Oliveira, B. G.; Hernandes, M. Z.; Rolim, L. A.; Rolim-Neto, P. J. The use of solid dispersion systems in hydrophilic carriers to increase benznidazole solubility. *J. Pharm. Sci.* **2011**, *100* (6), 2443−2451.
(44) Maniruzzaman, M.; Pang, J.; Morgan, D. J.; Douroumis, D. Molecular Modeling as a Predictive Tool for the Development of Solid Dispersions. *Mol. Pharmaceutics* **2015**, *12* (4), 1040−1049.
(45) Maniruzzaman, M.; Snowden, M. J.; Bradely, M. S.; Douroumis, D. Studies of intermolecular interactions in solid dispersions using advanced surface chemical analysis. *RSC Adv.* **2015**, *5* (91), 74212−74219.
(46) Shah, N.; Iyer, R. M.; Mair, H.-J.; Choi, D. S.; Tian, H.; Diodone, R.; Fähnrich, K.; Pabst-Ravot, A.; Tang, K.; Scheubel, E.; Grippo, J. F.; Moreira, S. A.; Go, Z.; Mouskountakis, J.; Louie, T.; Ibrahim, P. N.; Sandhu, H.; Rubia, L.; Chokshi, H.; Singhal, D.; Malick, W. Improved human bioavailability of vemurafenib, a practically insoluble drug, using an amorphous polymer-stabilized solid dispersion prepared by a solvent-controlled coprecipitation process. *J. Pharm. Sci.* **2013**, *102* (3), 967−981.
(47) Rodríguez-Hornedo, N.; Murphy, D. Surfactant-facilitated crystallization of dihydrate carbamazepine during dissolution of anhydrous polymorph. *J. Pharm. Sci.* **2004**, *93* (2), 449−460.
(48) Lehto, P.; Aaltonen, J.; Tenho, M.; Rantanen, J.; Hirvonen, J.; Tanninen, V. P.; Peltonen, L. Solvent-mediated solid phase transformations of carbamazepine: Effects of simulated intestinal fluid and fasted state simulated intestinal fluid. *J. Pharm. Sci.* **2009**, *98* (3), 985−996.
(49) Chen, J.; Ormes, J. D.; Higgins, J. D.; Taylor, L. S. Impact of surfactants on the crystallization of aqueous suspensions of celecoxib amorphous solid dispersion spray dried particles. *Mol. Pharmaceutics* **2015**, *12* (2), 533−541.
(50) Small, D. M., Size and Structure of Bile Salt Micelles. In *Molecular Association in Biological and Related Systems*; American Chemical Society: Washington, D.C., 1968; Vol. *84*, pp 31−52.
(51) Mandal, S.; Ghosh, S.; Banik, D.; Banerjee, C.; Kuchlyan, J.; Sarkar, N. An Investigation into the Effect of the Structure of Bile Salt Aggregates on the Binding Interactions and ESIHT Dynamics of Curcumin: A Photophysical Approach To Probe Bile Salt Aggregates as a Potential Drug Carrier. *J. Phys. Chem. B* **2013**, *117* (44), 13795−13807.
(52) Amundson, L. L.; Li, R.; Bohne, C. Effect of the Guest Size and Shape on Its Binding Dynamics with Sodium Cholate Aggregates. *Langmuir* **2008**, *24* (16), 8491−8500.
(53) Funasaki, N.; Fukuba, M.; Kitagawa, T.; Nomura, M.; Ishikawa, S.; Hirota, S.; Neya, S. Two-Dimensional NMR Study on the Structures of Micelles of Sodium Taurocholate. *J. Phys. Chem. B* **2004**, *108* (1), 438−443.
(54) Gomez-Mendoza, M.; Nuin, E.; Andreu, I.; Marin, M. L.; Miranda, M. A. Photophysical Probes To Assess the Potential of Cholic Acid Aggregates as Drug Carriers. *J. Phys. Chem. B* **2012**, *116* (34), 10213−10218.
(55) Natalini, B.; Sardella, R.; Gioiello, A.; Ianni, F.; Di Michele, A.; Marinozzi, M. Determination of bile salt critical micellization concentration on the road to drug discovery. *J. Pharm. Biomed. Anal.* **2014**, *87*, 62−81.
(56) Reis, S.; Moutinho, C. G.; Matos, C.; de Castro, B.; Gameiro, P.; Lima, J. L. F. C. Noninvasive methods to determine the critical micelle concentration of some bile acid salts. *Anal. Biochem.* **2004**, *334* (1), 117−126.
(57) Schwartz, A. M.; Myerson, A. S. 1 - Solutions and solution properties. In *Handbook of Industrial Crystallization*, 2nd ed.; Butterworth-Heinemann: Woburn, 2002; pp 1−31.
(58) Wiedmann, T. S.; Liang, W.; Kamel, L. Solubilization of Drugs by Physiological Mixtures of Bile Salts. *Pharm. Res.* **2002**, *19*, (8), 1203−1208.
(59) Carey, M. C. Bile Acids and Bile Salts: Ionization and Solubility Properties. *Hepatology* **1984**, *4* (S2), 66S−71S.
(60) Anwar, J.; Boateng, P. K.; Tamaki, R.; Odedra, S. Mode of Action and Design Rules for Additives That Modulate Crystal Nucleation. *Angew. Chem., Int. Ed.* **2009**, *48* (9), 1596−1600.
(61) Wuyts, B.; Brouwers, J.; Mols, R.; Tack, J.; Annaert, P.; Augustijns, P. Solubility Profiling of HIV Protease Inhibitors in Human Intestinal Fluids. *J. Pharm. Sci.* **2013**, *102* (10), 3800−3807.
(62) Hofmann, A. F.; Small, D. M. Detergent Properties of Bile Salts: Correlation with Physiological Function. *Annu. Rev. Med.* **1967**, *18* (1), 333−376.
(63) Wuyts, B.; Riethorst, D.; Brouwers, J.; Tack, J.; Annaert, P.; Augustijns, P. Evaluation of fasted and fed state simulated and human intestinal fluids as solvent system in the Ussing chambers model to explore food effects on intestinal permeability. *Int. J. Pharm.* **2015**, *478* (2), 736−744.
(64) Riethorst, D.; Mols, R.; Duchateau, G.; Tack, J.; Brouwers, J.; Augustijns, P. Characterization of Human Duodenal Fluids in Fasted and Fed State Conditions. *J. Pharm. Sci.* **2016**, *105* (2), 673−681.
(65) Pearson, P. J.; Parikh, S. *Review Article: Nature and Properties of Gastro-Oesophageal and Extra-Oesophageal Refluxate*; Blackwell: Oxford, ROYAUME-UNI, 2011; p 6.
(66) Vertzoni, M.; Fotaki, N.; Nicolaides, E.; Reppas, C.; Kostewicz, E.; Stippler, E.; Leuner, C.; Dressman, J. Dissolution media simulating the intralumenal composition of the small intestine: physiological issues and practical aspects. *J. Pharm. Pharmacol.* **2004**, *56* (4), 453−462.
(67) Roda, A.; Minutello, A.; Angellotti, M. A.; Fini, A. Bile acid structure-activity relationship: evaluation of bile acid lipophilicity using 1-octanol/water partition coefficient and reverse phase HPLC. *J. Lipid Res.* **1990**, *31* (8), 1433−43.
(68) Hofmann, A. F.; Roda, A. Physicochemical properties of bile acids and their relationship to biological properties: an overview of the problem. *J. Lipid Res.* **1984**, *25* (13), 1477−89.
(69) Matsuoka, K.; Suzuki, M.; Honda, C.; Endo, K.; Moroi, Y. Micellization of conjugated chenodeoxy- and ursodeoxycholates and solubilization of cholesterol into their micelles: comparison with other four conjugated bile salts species. *Chem. Phys. Lipids* **2006**, *139* (1), 1−10.
(70) Matsuoka, K.; Maeda, M.; Moroi, Y. Micelle formation of sodium glyco- and taurocholates and sodium glyco- and taurodeoxycholates and solubilization of cholesterol into their micelles. *Colloids Surf., B* **2003**, *32* (2), 87−95.

DOI: 10.1021/acs.cgd.6b01470
Cryst. Growth Des. XXXX, XXX, XXX−XXX